

# Explicit mean-field radius for nearly parallel vortex filaments in statistical equilibrium with applications to deep ocean convection

TIMOTHY D. ANDERSEN\*† and CHJAN C. LIM†

†Mathematical Sciences Dept., Rensselaer Polytechnic Institute, Troy, NY 12180

(September 2007)

Deep ocean convection, under appropriate conditions, gives rise to quasi-2D vortex structures with axes parallel to the rotational axis. These vortex structures appear in axisymmetric arrays that have a characteristic radius or size. This size is dependent, not only on competition between vortex interaction and conservation of angular momentum, but on 3D effects which many 2D models leave out. In this paper we propose a hypothesis that as 3D variations become more significant in these arrays, the process of interaction/angular momentum competition gives way to entropy/angular momentum competition and that this shift results in a reversal of the trend of the radius to decrease with increasing kinetic energy. We derive an explicit, closed-form, mean-field expression for the radius using a quasi-2D model for filaments with a local induction approximation (LIA). We validate the formula with Monte Carlo simulations. Both confirm that there is a reversal in the 2D contraction trend. We conclude that the proposed shift in competition does happen and that this simple LIA model is sufficient to show it.

*Keywords:* Deep ocean convection, quasi-2D vortex structures, statistical mechanics, Monte Carlo

## 1 Introduction

Deep ocean convection due to localised surface cooling is an important phenomenon that has been extensively studied in field observations (e.g. Greenland Sea), laboratory experiments, numerical, and theoretical models. In lab experiments on convective turbulence in homogeneous rotating fluids, a transition is observed from 3D turbulence to quasi-2D rotationally controlled vortex structures with axes parallel to the rotational axis (Maxworthy and Narimousa (1994), Raasch and Etling (1998)). When a large number of quasi-2D vortex structures are present, they can appear in arrays or lattices, and these have been commonly studied as fully-2D arrays, in one layer (Onsager (1949), Joyce and Montgomery (1973), Lim and Assad (2005)), or in two layers as a heton model (DiBattista and Majda (2001), Lim and Majda (2001)). However, it is an open question how quasi-2D structures nearer to the transition and/or with small inter-vortex distance behave because 2D models are not adequate to describe them. Of considerable interest is the relative cross-sectional size of these arrays—especially in terms of inter-vortex distance and curvature—that results from conservation of angular momentum (Majda and Wang (2006)).

In the statistical equilibrium model of Onsager (1949), rotational invariance provides an angular momentum constraint containing vortex structures close to the origin of the plane without boundaries, much as their are contained in the open ocean. In fact, Onsager’s model is one of the simplest non-integrable statistical mechanical models, making it interesting in a wide-range of fields from oceanography to condensed matter, and it is the simplest model for studying large numbers of vortex structures. Briefly, the Onsager model derives from the 2D Euler-equations for ideal fluids and is a Hamiltonian system such that, if there is a system of  $N$  point vortices (points of non-zero vorticity in the plane where vorticity is zero outside these points) with planar positions  $z_i$ ,  $i \in [1, N]$ , then

$$H_N^{2D} = - \sum_{j < k}^N \Gamma_j \Gamma_k \log |z_j - z_k|, \quad (1)$$

---

\*Corresponding Author Email: andert@alum.rpi.edu

where the vorticity at point  $z_j$  is  $\Gamma_j$  for all  $j$ . Because this Hamiltonian is rotational invariant, angular momentum is conserved, i.e.  $I_N^{2D} = \sum_{j=1}^N \Gamma_j |z_j|^2$  is constant. What this means is that if one vortex structure moves away from the origin, another must move closer to restore the balance. Assuming that no two structures are allowed to be in exactly the same position in the plane, no structure may move away to infinity. Onsager further postulated that the following **canonical** distribution could describe the statistics of the system of vortex structures:

$$P_N^{2D}(s) = \frac{1}{Z_N^{2D}} e^{-\beta H_N - \mu I_N}, \tag{2}$$

where  $Z_N^{2D} = \sum_s e^{-\beta H_N - \mu I_N}$ ,  $s$  is a set of vortex positions  $\{z_j\}$  and strengths  $\{\Gamma_j\}$ ,  $\beta$  and  $\mu$  are Lagrange multipliers, the first determining the kinetic energy of the reservoir, called **inverse temperature**, and the second the angular momentum of the reservoir, called **chemical potential**. (In this case the reservoir is the fluid external to the convection-driven vortex structures such as the surrounding ocean water.) This model combines minimal information about fluid behavior and vortex interaction making it useful if not analytically solvable.

The trouble with this model is that it is entirely two dimensional, neglecting all 3D effects, which become exceptionally important when rotation is weak or counter-currents are strong, and so extensions have been made to introduce 3-dimensionality without losing the advantages of the 2D logarithmic interaction and without resorting to complete 3D turbulence modelling. One such attempt is the equilibrium statistical model of DiBattista and Majda (2001) (applied specifically to deep ocean convection in Lim and Majda (2001)) which proposes layering two 2D Point Vortex Gases one on top of the other and introducing interaction between layers giving a pseudo-3D flavour. This slightly more complicated model has allowed for some interesting results in determining the statistical distribution of vortices in the layers from low-interaction levels where the distribution is essentially normal to high-interaction where it is essentially uniform with a sharp cut-off at the boundary Assad and Lim (2006).

An extension of the two layered approach is a multi-layered approach, and, taking this approach to its logical conclusion, we arrive at what one could term the “infinite”-layered model but what is more commonly called the nearly parallel vortex filament model (Klein et al. (1995), Lions and Majda (2000)). This is the model studied in this paper; therefore, we devote §2 to explaining it more completely. To outline it briefly here, it is a model in which the 3D vorticity field is represented as a large number,  $N$ , of vortex filaments. Each vortex filament,  $j$ , is a curve in space that we represent as a complex function,  $\psi_j(\sigma) \in \mathbb{C}$ , where  $\sigma \in \mathbb{R}$  is a parameter, and each one has a certain strength  $\lambda_j$ . The vortex curves are all nearly parallel (in an asymptotic sense) to the  $z$ -axis, hence, *nearly parallel* vortex filaments. Because they are quasi-2D, they have a 2D interaction between points in the same plane on different filaments. Stretching is minimal. Internal fluctuations are represented with a local-induction approximation (LIA), explained in §2. The best benefit of the system is that it is finite Hamiltonian and fits into the same distribution as the original Onsager model. Since our investigation into 3D effects are based on theoretical analysis of the probability distribution and Monte Carlo simulations, this simplicity is crucial.

In our analysis of the equilibrium statistics of this system, we focus on the most critical statistic: size, defined as the second moment of the statistical distribution (§2). Size is important in the study of ocean convection because, of all statistical behaviours, it is the most visible and the most measurable. Clearly, the third dimensional variations in filaments have some effect on overall system size, but it is an open question whether there is a phase transition due to increasing 3D effects in a quasi-2D system and whether the local self-induced variations act as a counter to the expansive effect of interaction potential or challenge the squeezing effect of conservation of angular momentum. To determine this, we set our goal to achieving an explicit, closed-form approximation for the system size and confirming its accuracy computationally.

In order to determine the size of the system analytically, we use a mean-field approach, described in §3, in which the system of  $N$  vortex filament structures is replaced with two vortex filaments, an ordinary one a mean distance from the origin with strength 1 and a perfectly straight one at the origin containing the mean centre of vorticity (having a strength of  $N - 1$ ). We use the statistics of the outer vortex to approximate the behavior of any given vortex in the system. Our approximation is a special case of the

rigorous mean-field approach of Lions and Majda (2000) and is justified in its existence. To justify its accuracy, we turn to Monte Carlo simulations of the original system, described in §5.

Our results indicate that not only is the mean-field approximation surprisingly accurate given its crudeness but that the size of the system experiences a significant transition in the parameter  $\beta$ . We find that a  $\beta_0$  exists such that the change in the size with respect to  $\beta$  switches direction. We are able to calculate an explicit, closed-form formula for the squared size of the system,  $R^2$ , (§C) and confirm the formula with Monte Carlo measurements (§5).

## 2 The Nearly Parallel Vortex Filament Model's Entropy-Driven Shift

### 2.1 Background

The full boundary value problem of deep ocean convection-driven vortex structures is exceedingly complicated and not necessarily useful. To extract general physical principles the full complexity is not required. Rather, the Onsager model and its related models (Onsager (1949), Assad and Lim (2006)) simplify the 2D Euler problem to the bare minimum required for a meaningful statistical mechanical approach: no boundaries, discrete vortex structures with no individual cross-sections (points), and a large number of conserved quantities such as energy, angular momentum, vorticity, etc. Leaving out 3D effects, these models fail in cases where inter-vortex distance is small relative to the distance a filament's curve travels in the plane. (Filaments are able to cross each other due to their internal viscosity which is not represented explicitly in inviscid models.) The nearly parallel vortex filament model adds a small element of true 3-dimensionality to the 2D Point-Vortex Gas, enough to explore what happens when plane-position variations along the filament begin to dominate vortex-vortex interaction and angular momentum.

Without describing the mathematics in detail yet, 3D vortex filaments behave much like springs, and stretching the filament increases its energy. In systems of nearly parallel vortex filaments, there are two kinds of energy: self-energy that increases with localised stretching and interaction energy that increases as vortex structures come closer together. The other component, angular momentum, is conserved but unaffected by temperature. Because the convective-rotation is nearly a rigid rotation, angular momentum increases with the square of distance from the axis of rotation (the  $z$ -axis in our case). When the self-energy is insignificant (or zero), the interaction energy and angular momentum compete and determine the system's size.

For the case of zero self-energy (and zero entropy) Lim and Assad (2005) give a formula for the system size,

$$R^2 = \frac{\Lambda\beta}{4\mu}, \quad (3)$$

where

$$R^2 = \lim_{N \rightarrow \infty} \int ds N^{-1} \sum_{j=1}^N |z_j|^2 p(s), \quad (4)$$

is the second-moment of  $p(s) = P_N^{2D}(s)$  in the infinite- $N$  limit with the necessary redefinition of inverse temperature,  $\beta' = \beta N$  where  $\beta'$  is kept constant (called a **non-extensive thermodynamic limit**), and  $\Lambda$  is the total vortex strength, also kept constant in  $N$ .

### 2.2 Hypothesis

Our hypothesis is that when filament variations become large compared to inter-vortex distance the following process becomes dominant: when a vortex moves away from the centre, potential energy decreases and angular momentum increases. In a 2D model this would cause other vortices to move inward to restore

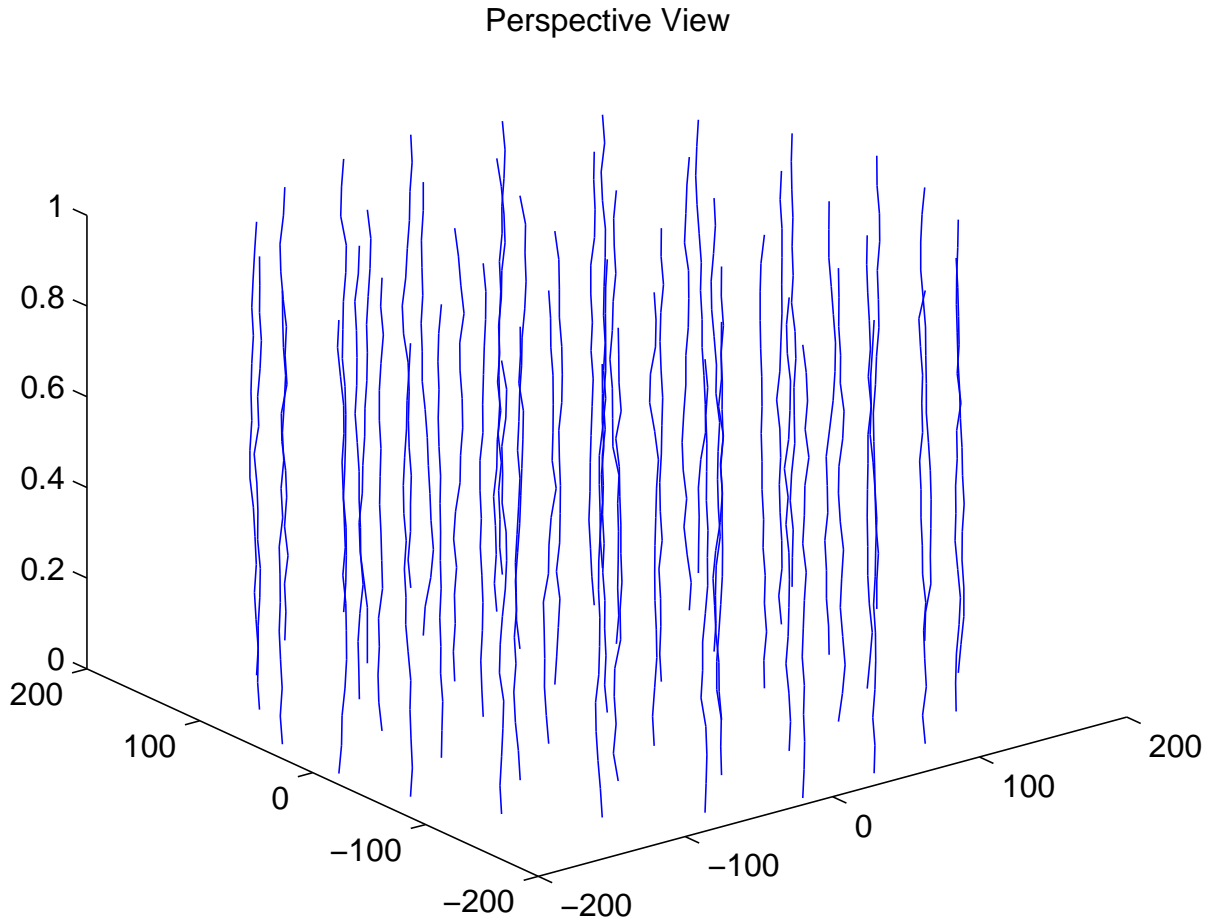


Figure 1. This output from our Monte Carlo simulation of a single sample illustrates how the moderate-temperature nearly parallel vortex filament model appears. In a high-temperature case, filaments may cross while in low-temperature cases the filaments' variations are too small to be visible.

the balance (Process 1). In a 3D model, this can also happen, but, alternatively, part of the *same filament* can move closer to the centre, leaving the other filaments fixed (Process 2). This increase in variation restores the balance but increases the self-energy, so the change towards the centre is not as significant as it would be if a different filament moved to compensate. The overall effect of Process 2 is expansion. Process 1 results in a lower total energy than Process 2 and so, at low positive temperatures, this is the dominating process, but, at high positive temperatures, Process 2 dominates because Process 1 does not increase the entropy of the system, while Process 2 does. Thus, the shift from Process 1 to Process 2 is entropy driven.

As entropy becomes more significant, this expansive effect begins to dominate. We hypothesise that as the cost of increasing self-energy and interaction energy (the total energy) decreases with increasing temperature, a double effect occurs: the angular momentum contracts the system, decreasing inter-vortex distance at first, but the decreased distance causes the variations become more significant without making the filaments any less straight. The expansion effect begins to dominate the angular momentum's contraction effect, eventually stopping and reversing the contraction of the system's size. Showing that this occurs would effectively validate the hypothesis. However, we go one step further and give an explicit formula for  $R^2$ , which allows us to explore the parameter space as completely as possible.

### 2.3 Mathematical Model

With our hypothesis given, the following is an overview of the mathematical model we employ: This quasi-2D model, (Klein et al. (1995)) is derived rigorously from the Navier-Stokes equations and represents vorticity as a bundle of  $N$  filaments that are nearly parallel to the  $z$ -axis. The model has a Hamiltonian,

$$H_N = \alpha \int_0^L d\sigma \sum_{k=1}^N \frac{1}{2} \left| \frac{\partial \psi_k(\sigma)}{\partial \sigma} \right|^2 - \int_0^L d\sigma \sum_{k=1}^N \sum_{i>k}^N \log |\psi_i(\sigma) - \psi_k(\sigma)|, \quad (5)$$

where  $\psi_j(\sigma) = x_j(\sigma) + iy_j(\sigma)$  is the position of vortex  $j$  at position  $\sigma$  along its length, the circulation constant is same for all vortices and set to 1, and  $\alpha$  is the core structure constant (Klein et al. (1995)). The position in the complex plane,  $\psi_j(\sigma)$ , is assumed to be periodic in  $\sigma$  with period  $L$ . The angular momentum is

$$I_N = \sum_i^N \int_0^L d\sigma |\psi_i(\sigma)|^2. \quad (6)$$

The Gibbs distribution for this system,  $P_N$ , has the same form as  $P_N^{2D}$ :

$$P_N(s) = \frac{1}{Z_N} e^{-\beta H_N - \mu I_N}, \quad (7)$$

where  $Z_N = \sum_s e^{-\beta H_N - \mu I_N}$ .

### 3 A Simple Mean-field Theory

The first step in any paper analysis of a statistical mechanical system is to calculate or approximate the normalising factor,  $Z_N$ , called the **partition function**. The partition function for the quasi-2D system,

$$Z_N = \int D\psi_1 \cdots \int D\psi_N \exp(S_N), \quad (8)$$

where  $D\psi_i$  represents functional integration over all paths for each filament  $i$  (also known as a Feynman or Feynman-Kac integral, Feynman and Wheeler (1948)). The functional  $S_N = -\beta H_N - \mu I_N$  is the **action**.

We have the most-probable free energy from the following formula (Schrödinger (1952)):

$$F = -\frac{1}{\beta} \log Z_N. \quad (9)$$

As is well-known, the state that gives the minimum free energy is the most-probable state of the system. In this case the state consists of the positions of the filaments  $\{\psi_i\}_{i=1\dots N}$ . The interaction term (second term in Equation 5) makes a direct analytical solution impossible with current knowledge. While the other terms in  $S_N$ , the self-induction (from the first term in Eq. 5) and the conservation of angular momentum term,  $-\mu I_N$ , are negative definite quadratic and yield a normally distributed Gibbs distribution that we can functionally integrate, the logarithmic term must be approximated. The simplest way to do the approximation is a mean-field theory which will reduce the problem from  $N$  coupled (interacting) filaments to  $N$  uncoupled (non-interacting) filaments.

Although Lions and Majda (2000) have made such an approximation and rigorously derived a mean-field evolution PDE for the probability distribution of the vortices in the complex plane, their PDE takes the form of a non-linear Schrödinger equation that is not analytically solvable (even in equilibrium), again because of the interaction term. Our mean-field theory is a special case of theirs.

A reasonable approach to a mean-field theory is to change the interaction between each filament and all the other filaments to an interaction between a single filament and one perfectly straight filament at the origin with the combined strength of all the filaments. Each pair of filaments  $i$  and  $j$  have a square distance associated with each plane  $\sigma$ :  $|\psi_i(\sigma) - \psi_j(\sigma)|^2$ . Because the system is axisymmetric with centre at the origin, the mean square distance between a filament and any other filament is the square distance between that filament and the origin. If we take  $\langle \cdot \rangle$  to mean average, then  $\langle |\psi_i(\sigma) - \psi_j(\sigma)|^2 \rangle \approx |\psi_i(\sigma)|^2$  where the average is over filaments  $j$ . (We say “ $\approx$ ” because the average is only exact for infinite  $N$ .) Furthermore, the mean square distance of a filament from the origin,  $\langle |\psi_i|^2 \rangle = N^{-1} \sum_{i=1}^N \int_0^L d\sigma |\psi_i(\sigma)|^2 = N^{-1} I_N$ . Given these assumptions the interaction takes the following form:

$$\int_0^L d\sigma \frac{1}{4} \sum_{i=1}^N \sum_{j=1}^N \log |\psi_i(\sigma) - \psi_j(\sigma)|^2 = \frac{N^2}{4} \log \frac{I_N}{N} \quad (10)$$

Therefore, we can take the mean-field action to be

$$S_N^{mf} = \frac{LN^2\beta}{4} \log \frac{I_N}{N} - \int_0^L d\sigma \left[ \sum_{k=1}^N \frac{\beta\alpha}{2} \left| \frac{\partial \psi_k(\sigma)}{\partial \sigma} \right|^2 + \mu \sum_{k=1}^N |\psi_k(\sigma)|^2 \right], \quad (11)$$

where the first term is now mean-field and the other two are the same as before.

Before we begin to calculate the partition function, we must deal with another problem: we still cannot integrate Equation 8 using this action because the interaction term is still a function of  $\psi$ , so we make another approximation, adding a spherical constraint (Berlin and Kac (1952), Hartman and Weichman (1995)) on the angular momentum,

$$\delta \left( \int_0^L d\sigma [I_N - NR^2] \right), \quad (12)$$

that has integral representation,

$$\int_{-\infty+i\tau_0}^{\infty+i\tau_0} \frac{d\tau}{2\pi} \exp \int_0^L -i\tau [I_N - NR^2], \quad (13)$$

where  $R^2$  is defined by Equation 4. The spherical-mean-field partition function is now

$$Z_N^{smf} = \int D\psi_1 \cdots \int D\psi_N \exp \left( S_N^{mf} \right) \int_{-\infty}^{\infty} \frac{d\tau}{2\pi} \exp \int_0^L d\sigma - i\tau [I_N - NR^2]. \quad (14)$$

The spherical constraint does not alter the statistics of the system significantly because the angular momentum already has an implicit preferred value,  $NR^2$ , we are simply making it explicit.

#### 4 Solving for $R^2$

We now solve  $Z_N^{smf}$  in closed-form in the limit as  $N \rightarrow \infty$ : Since the exponents are all negative definite, we can interchange the integrals and combine exponents,

$$Z_N^{smf} = \int \frac{d\tau}{2\pi} \int D\psi_1 \cdots \int D\psi_N \exp \left( S_N^{smf} \right). \quad (15)$$

where the combined action functional is  $S_N^{smf} = \sum_{k=1}^N S_k$ , and the single filament action is

$$S_k = \left[ \beta L N \log(R^2)/4 - \frac{1}{2} \int_0^L d\sigma \alpha \beta \left| \frac{\partial \psi_k(\sigma)}{\partial \sigma} \right|^2 + (i\tau + 2\mu) |\psi_k(\sigma)|^2 - iR^2 \tau \right]. \quad (16)$$

Because  $\{\psi_k\}$  are statistically independent for all  $k$ , we can drop the  $k$  subscript. Therefore, the total action is simply a multiple of the single filament action:  $S_N^{smf} = NS$ , which makes the partition function,

$$Z_N^{smf} = \int \frac{d\tau}{2\pi} \left\{ \int D\psi \exp S \right\}^N. \quad (17)$$

Now we define the **non-dimensional free energy**,  $f[i\tau] = \beta F$ . Using the formula in Equation 9,

$$f[i\tau] = -\log \left[ \int D\psi \exp(S) \right] \quad (18)$$

and

$$Z_N^{smf} = \int_{-\infty}^{\infty} \frac{d\tau}{2\pi} \exp(-Nf[i\tau]). \quad (19)$$

We now have a partition function we can solve with steepest-descent methods if we find an expression for  $f$ . The functional  $f[i\tau]$  is the energy of a 2-D quantum harmonic oscillator with a constant force and simply evaluated with Green's function methods (not given here) (Brown (1992)).

Let  $\lambda = i\tau + 2\mu$ ,  $\beta' = \beta N$  and  $\alpha' = \alpha/N$ . After evaluating the integral, Equation 18, (done in Appendix C), the free-energy reads

$$f[\lambda] = L\mu - \frac{1}{2} L\lambda R^2 - \beta' L \log(R^2)/4 - \ln \frac{e^{-\omega L}}{(e^{-\omega L} - 1)^2}, \quad (20)$$

where  $\omega = \sqrt{\lambda/(\alpha'\beta')}$  is the harmonic oscillator frequency.

Now that we have a formula for  $f$  we can apply the saddle point or steepest descent method. (For discussion of this method see Appendix B as well as the original paper of Berlin and Kac (Berlin and Kac (1952)).) The intuition is that, as  $N \rightarrow \infty$  in the partition function, only the minimum energy will contribute to the integral, i.e. at infinite  $N$ , the exponential behaves like a Dirac delta function, so

$$f_\infty = \lim_{N \rightarrow \infty} -\frac{1}{N} \ln Z_N^{smf} = f[\eta], \quad (21)$$

where  $\eta$  is such that  $\partial f[\lambda]/\partial \lambda|_\eta = 0$  (Hartman and Weichman (1995), Berlin and Kac (1952)).

First we can make a simplification by ridding Equation 20 of  $R^2$ . We know that  $R^2$  will minimise  $f$  and so  $\partial f/\partial R^2 = 0$ . Therefore,

$$R^2 = \frac{\beta'}{4(\mu - \lambda/2)}. \quad (22)$$

Substituting the left side of 22 for  $R^2$  in Equation 20, we get

$$f[\lambda] = \beta' L/4 + \sqrt{\frac{\lambda}{\alpha'\beta'}} L + 2 \log \left| \exp \left( -\sqrt{\frac{\lambda}{\alpha'\beta'}} L \right) - 1 \right| - \frac{\beta' L}{4} \log \frac{\beta'}{4(\mu - \lambda/2)}. \quad (23)$$

We could take the derivative of Equation 23 and set it equal to zero to obtain  $\eta$ . However, doing so yields a transcendental equation that needs to be solved numerically. Since our goal is to obtain an explicit formula, we choose to study the system as  $L \rightarrow \infty$ . In fact such an approach is justified by the assumptions of the model that  $L$  have larger order than the rest of the system's dimensions. (If this were a quantum system, this procedure would be equivalent to finding the energy of the ground state. Hence, we call this energy  $f_{grnd}$ .) Taking the limit on Equation 23 yields the free energy per unit length in which  $\eta$  can be solved for

$$f_{grnd}[\eta] = \frac{\beta'}{4} + \sqrt{\eta/(\alpha'\beta')} - \frac{\beta'}{4} \log \left( \frac{\beta'}{4(\mu - \eta/2)} \right), \quad (24)$$

where

$$\eta = 2\mu - \frac{1}{8}\beta'(-\beta'^2\alpha' + \sqrt{\beta'^4\alpha'^2 + 32\alpha'\beta'\mu}) \quad (25)$$

gives physical results.

With  $\eta$  explicit, we can give a full formula for  $R^2$ ,

$$R^2 = \frac{\beta'^2\alpha' + \sqrt{\beta'^4\alpha'^2 + 32\alpha'\beta'\mu}}{8\alpha'\beta'\mu}. \quad (26)$$

Through several approximations, we have obtained an explicit formula for the free energy of the system and  $R^2$ .

## 5 Monte Carlo Comparison

We apply Monte Carlo in this paper to the original quasi-2D model with Hamiltonian 5 to verify two hypotheses:

- (i) that the 3-D effects, namely the Equation 26, predicted in the mean-field are correct
- (ii) that these effects can be considered physical in the sense that the model's asymptotic assumptions of straightness is not violated.

Research on flux-lines in type-II superconductors has yielded a close correspondence between the behavior of vortex filaments in 3-space and paths of quantum bosons in (2+1)-D (2-space in imaginary time) (Nordborg and Blatter (1998), Sen et al. (2001)). This work is not related to ours fundamentally because type-II superconductor flux-lines do not have the same boundary conditions. They use periodic boundaries in all directions with an interaction cut-off distance while we use no boundary conditions and no cut-off. Besides the boundaries, they also allow flux-lines to permute like bosons, switching the top end points, which we do not allow for our vortices. However, despite the boundary differences, the London free-energy functional for interacting flux-lines is closely related to our Hamiltonian 5, and so we can apply Path Integral Monte Carlo (PIMC) in the same way as it has been applied to flux-lines. (For a discussion of PIMC and how we apply it see Appendix A.)

We simulated a collection of  $N = 20$  vortices each with a piecewise linear representation with  $M = 1024$  segments and ran the system to equilibration, determined by the settling of the mean and variance of the total energy. We ran the system for 20 logarithmically spaced values of  $\beta$  between 0.001 and 1 plus two points, 10 and 100. We set  $\alpha = 10^7$ ,  $\mu = 2000$ , and  $L = 10$ . We calculate several arithmetic averages: the mean square vortex position,

$$R_{MC}^2 = (MN)^{-1} \sum_{i=1}^N \sum_{k=1}^M |\psi_i(k)|^2, \quad (27)$$

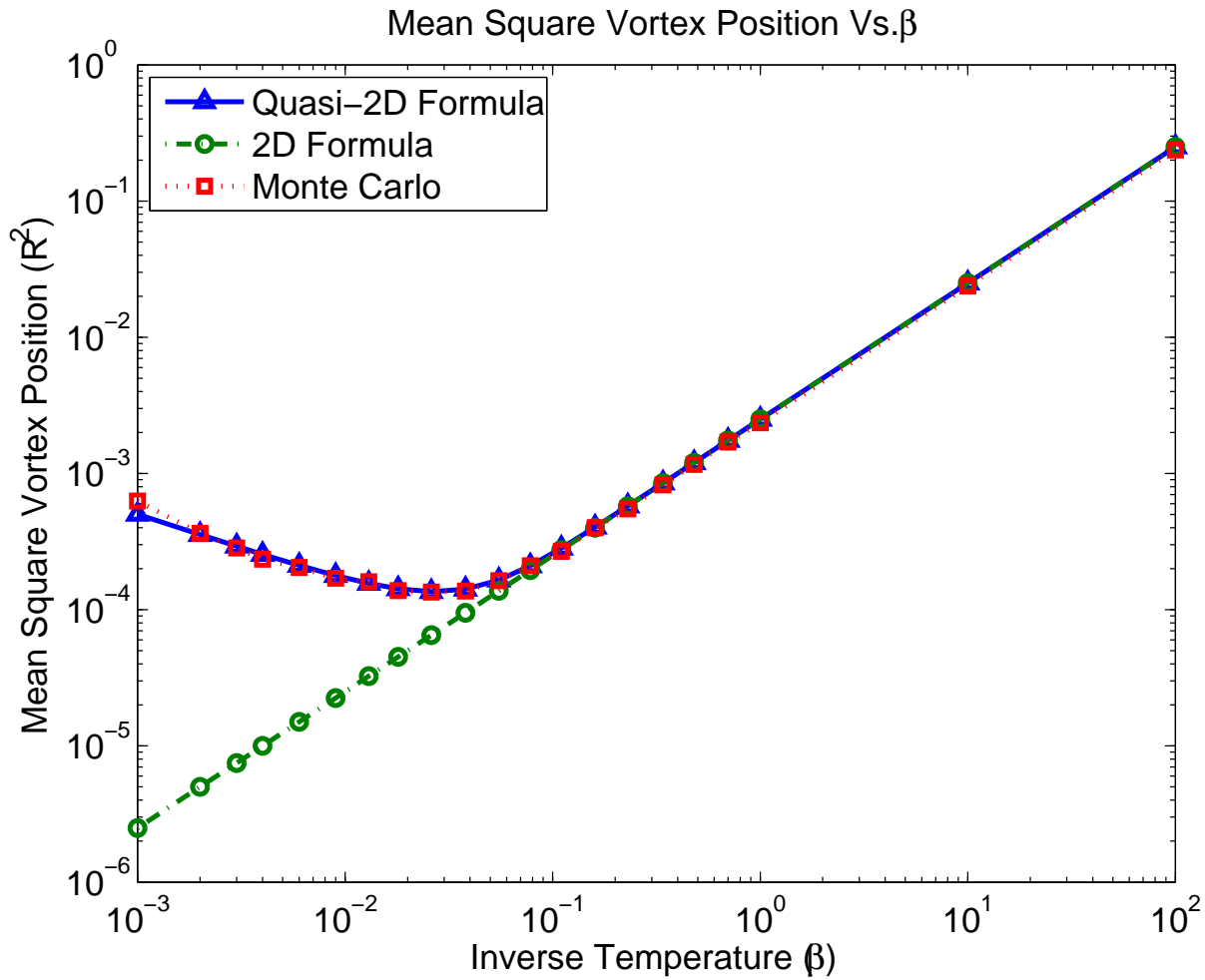


Figure 2. The mean square vortex position, defined in Equation 27, compared with Equations 26 and 3 shows how 3-D effects come into play around  $\beta = 0.16$ . That the 2D formula continues to decrease while the Monte Carlo and the quasi-2D formula curve upwards with decreasing  $\beta$  suggests that the internal variations of the vortex lines have a significant effect on the probability distribution of vortices.

where  $k$  is the segment index corresponding to discrete values of  $\sigma$ , and the mean square amplitude per segment,

$$a^2 = (MN)^{-1} \sum_{i=1}^N \sum_{k=1}^M |\psi_i(k) - \psi_i(k+1)|^2, \quad (28)$$

where  $\psi_i(M+1) = \psi_i(1)$ .

Measures of Equation 27 correspond well to Equation 26 in Figure 2 whereas Equation 3 continues to decline when the others curve with decreasing  $\beta$  values, suggesting that the 3-D effects are not only real in the Monte Carlo but that the mean-field is a good approximation with these parameters.

In order to be considered straight enough, we need

$$a \ll \frac{L}{M} = \frac{10}{1024}. \quad (29)$$

Straightness holds for all  $\beta$  values, shown in Figure 3 as slope. We do not need to show that these conditions hold for every instance in the Monte Carlo, only close to the average, because small probability events have little effect on the statistics.

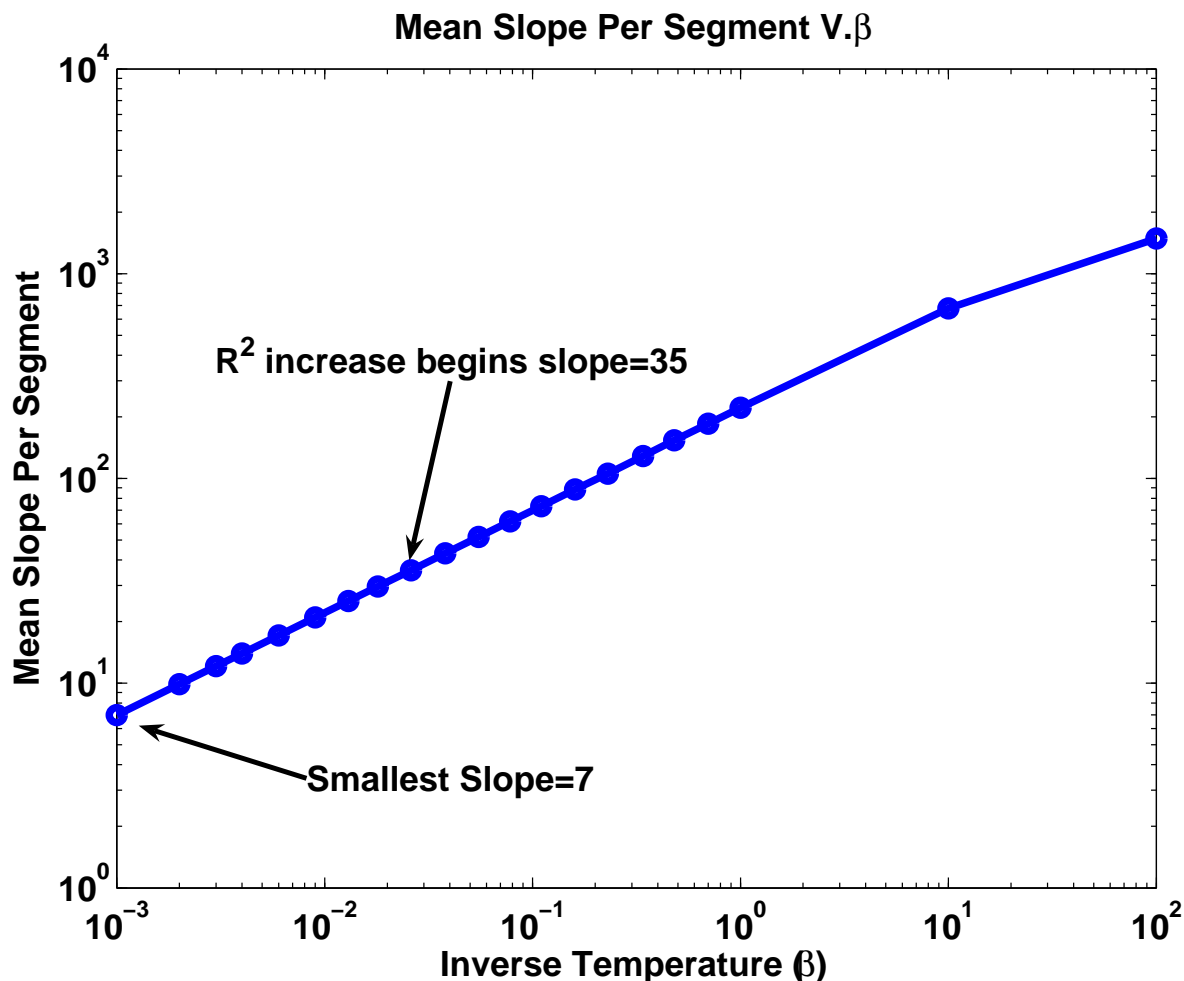


Figure 3. This figure shows the segment height  $L/M = 10/1024$  divided by the mean amplitude per segment (Equation 28), i.e. the mean slope per segment. The smallest slope is 7 (quite straight at about  $82^\circ$ ) indicating that straightness constraints hold for all  $\beta$  values.

## 6 Related Work

The closest study to this is the heton model study of Lim and Majda (2001) which applied a two layered vortex model to deep ocean convection. However, a two layered model is insufficient to show the effects we have shown.

As mentioned in the previous section, simulations of flux lines in type-II superconductors using the PIMC method have been done, generating the Abrikosov lattice (Nordborg and Blatter (1998), Sen et al. (2001)). However, the superconductor model has periodic boundary conditions in the  $xy$ -plane, is a different problem altogether, and is not applicable to trapped fluids. No Monte Carlo studies of the model of Klein et al. (1995) have been done to date and dynamical simulations have been confined to a handful of vortices. Kevlahan (2005) added a white noise term to the KMD Hamiltonian, Equation 5, to study vortex reconnection in comparison to direct Navier-Stokes, but he confined his simulations to two vortices. Direct Navier-Stokes simulations of a large number of vortices are beyond our computational capacities.

Tsubota et al. (2003) has done some excellent simulations of vortex tangles in He-4 with rotation, boundary walls, and *ad hoc* vortex reconnections to study disorder in rotating superfluid turbulence. Because vortex tangles are extremely curved, they applied the full Biot-Savart law to calculate the motion of the filaments in time. Their study did not include any sort of comparison to 2-D models because for most of the simulation vortices were far too tangled. The inclusion of rigid boundary walls, although correct for the study of He-4, also makes the results only tangentially applicable to the KMD system we use.

Our use of the spherical model is recent and has also been applied to the statistical mechanics of macroscopic fluid flows in order to obtain exact solutions for quasi-2D turbulence (Lim and Nebus (2006), Lim (2006)).

Other related work on the statistical mechanics of turbulence in 3-D vortex lines can be found in Flandoli and Gubinelli (2002) and Berdichevsky (1998) in addition to Lions and Majda (2000).

## 7 Conclusion

We have developed an explicit mean-field formula for the most significant statistical moment for the quasi-2D model of nearly parallel vortex filaments and shown that in Monte Carlo simulations this formula agrees well while the related 2-D formula fails at higher temperatures. We have also shown that our predictions do not violate the model's asymptotic assumptions for a range of inverse temperatures. Therefore, we conclude that these results are likely physical. We consider this strong evidence supporting our original hypothesis.

The implication towards deep ocean convection is that 3D effects become significant when vortex structures move close together and that this, ultimately causes an expansion in the system size that one would not see in more 2D structures. However, although the system as a whole expands, we cannot say whether this expansion is uniform or if there is a separation effect in which a small core surrounded by a halo of vortex structures emerges. Knowing that could have significant implications for the understanding of these structures.

## Appendix A: Path Integral Monte Carlo method

Path Integral Monte Carlo methods emerged from the path integral formulation invented by Dirac that Richard Feynman later expanded (Zee (2003)), in which particles are conceived to follow all paths through space. One of Feynman's great contributions to the quantum many-body problem was the mapping of path integrals onto a classical system of interacting "polymers" (Feynman and Wheeler (1948)). D. M. Ceperley used Feynman's convenient piecewise linear formulation to develop his PIMC method which he successfully applied to He-4, generating the well-known lambda transition for the first time in a microscopic particle simulation (Ceperley (1995)). Because it describes a system of interacting polymers, PIMC applies to classical systems that have a "polymer"-type description like nearly parallel vortex filaments.

PIMC has several advantages. It is a *continuum* Monte Carlo algorithm, relying on no spatial lattice. Only time (length in the z-direction in the case of vortex filaments) is discretised, and the algorithm makes no assumptions about types of phase transitions or trial wavefunctions.

For our simulations we assume that the filaments are divided into an equal number of segments of equal length. This discretisation leads to the Hamiltonian,

$$H_N(M) = H_N^{self}(M) + H_N^{int}(M) \quad (\text{A1})$$

where

$$H_N^{self} = \alpha \sum_{j=1}^M \sum_{k=1}^N \frac{1}{2} \frac{|\psi_k(j+1) - \psi_k(j)|^2}{\delta} \quad (\text{A2})$$

and

$$H_N^{int} = - \sum_{j=1}^M \sum_{k=1}^N \sum_{i>k}^N \delta \log |\psi_i(j) - \psi_k(j)|, \quad (\text{A3})$$

and angular momentum

$$I_N = \sum_{j=1}^M \sum_{k=1}^N \delta |\psi_k(j)|^2, \quad (\text{A4})$$

where  $\delta$  is the length of each segment,  $M$  is the number of segments, and  $\psi_k(j) = x_k(j) + iy_k(j)$  is the position of the point at which two segments meet (called in PIMC a ‘‘bead’’) in the complex plane.

The probability distribution for vortex filaments,

$$G_N(M) = \frac{\exp(-\beta H_N(M) - \mu I_N(M))}{Z_N(M)}, \quad (\text{A5})$$

where

$$Z_N(M) = \sum_{\text{allpaths}} G_N(M), \quad (\text{A6})$$

is the Gibbs canonical distribution. Our Monte Carlo simulations sample from this distribution.

The Monte Carlo simulation begins with a random distribution of filament end-points in a square of side 10, and there are two possible moves that the algorithm chooses at random. The first is to move a filament’s end-points. A filament is chosen at random, and its end-points moved a uniform random distance. Then the energy of this new state,  $s'$ , is calculated and retained with probability

$$A(s \rightarrow s') = \min \{1, \exp(-\beta[H_N^{\text{int}}(s') - H_N^{\text{int}}(s)] - \mu[I_N(s') - I_N(s)])\}, \quad (\text{A7})$$

where  $s$  is the previous state. (Self-induction,  $H_N^{\text{self}}$ , is unchanged for this type of move since it is internal to each filament.) The second move keeps end-points stationary and, following the bisection method of Ceperley, grows a new internal configuration for a randomly chosen filament (Ceperley (1995)). Both the self-induction and the trapping potential are harmonic, so the Gibbs canonical distribution without interaction can be sampled directly as a Gaussian distribution. Therefore, in this move the configuration is generated by first sampling a free vortex filament, and then accepting the new state with probability

$$A(s \rightarrow s') = \min \{1, \exp[-\beta(H_N^{\text{int}}(s') - H_N^{\text{int}}(s))]\}. \quad (\text{A8})$$

Our stopping criteria is graphical in that we ensure that the cumulative arithmetic mean of the energy settles to a constant. Typically, we run for 10 million moves or 50,000 sweeps for 200 vortices. Afterwards, we collect data from about 200,000 moves to generate statistical information.

## Appendix B: Spherical Model and the Saddle Point Method

The spherical model was first proposed in a seminal paper of Berlin and Kac (Berlin and Kac (1952)), in which they were able to solve for the partition function of an Ising model given that the site spins satisfied a spherical constraint, meaning that the squares of the spins all added up to a fixed number. The method relies on what is known as the saddle point or steepest descent approximation method which is exact only for an infinite number of lattice sites.

In general the steepest descent or saddle-point approximation applies to integrals of the form

$$\int_a^b e^{-Nf(x)} dx, \quad (\text{B1})$$

where  $f(x)$  is a twice-differentiable function,  $N$  is large, and  $a$  and  $b$  may be infinite. A special case, called Laplace's method, concerns real-valued  $f(x)$  with a finite minimum value.

The intuition is that if  $x_0$  is a point such that  $f(x_0) < f(x) \forall x \neq x_0$ , i.e. it is a global minimum, then, if we multiply  $f(x_0)$  by a number  $N$ ,  $Nf(x) - Nf(x_0)$  will be larger than just  $f(x) - f(x_0)$  for any  $x \neq x_0$ . If  $N \rightarrow \infty$  then the gap is infinite. For such large  $N$ , the only significant contribution to the integral comes from the value of the integrand at  $x_0$ . Therefore,

$$\lim_{N \rightarrow \infty} \left[ \int_a^b e^{-Nf(x)} dx \right]^{1/N} = e^{-f(x_0)}, \quad (\text{B2})$$

or

$$\lim_{N \rightarrow \infty} -\frac{1}{N} \log \int_a^b e^{-Nf(x)} dx = f(x_0), \quad (\text{B3})$$

(Berlin and Kac (1952), Hartman and Weichman (1995)). A proof is easily obtained using a Taylor expansion of  $f(x)$  about  $x_0$  to quadratic degree.

### Appendix C: Evaluating the Free Energy Integral

In this section we discuss our evaluation of the integral

$$f[i\tau] = -\log \left[ \int D\psi \exp(S) \right], \quad (\text{C1})$$

where

$$S = \left[ \beta' L \log(R^2)/4 - \frac{1}{2} \int_0^L d\sigma \alpha' \beta' \left| \frac{\partial \psi(\sigma)}{\partial \sigma} \right|^2 + (i\tau + 2\mu) |\psi(\sigma)|^2 - iR^2 \tau \right], \quad (\text{C2})$$

$\beta' = \beta N$ , and  $\alpha' = \alpha N^{-1}$ .

The free-energy, Equation C1, involves a simple harmonic oscillator with a constant external force, and we can re-write it,

$$f[i\tau] = -\frac{1}{2} i\tau L R^2 - \beta' L \log(R^2)/4 - \ln h[i\tau]. \quad (\text{C3})$$

Here  $h$  is the partition function for a quantum harmonic oscillator in imaginary time,

$$h[i\tau] = \int D\psi \exp \left( \int_0^L d\sigma - \frac{1}{2} m [|\partial_\sigma \psi|^2 + \omega^2 |\psi|^2] \right), \quad (\text{C4})$$

which has the well-known solution for periodic paths in (2+1)-D where we have integrated the end-points over the whole plane as well,

$$h[i\tau] = \frac{e^{-\omega L}}{(e^{-\omega L} - 1)^2}, \quad (\text{C5})$$

where  $m = \alpha' \beta'$  and  $\omega^2 = (i\tau + 2\mu)/(\alpha' \beta')$  (Brown (1992), Zee (2003)).

Let us make a change of variables  $\lambda = i\tau + 2\mu$ . Then the free-energy reads

$$f[\lambda] = \left(\mu - \frac{1}{2}\lambda\right)LR^2 - \beta' L \log(R^2)/4 - \ln \frac{e^{-\omega L}}{(e^{-\omega L} - 1)^2}, \quad (\text{C6})$$

where  $\omega = \sqrt{\lambda/(\alpha'\beta')}$ .

#### **Acknowledgements**

This work is supported by ARO grant W911NF-05-1-0001 and DOE grant DE-FG02-04ER25616.

## REFERENCES

- Assad, S. M. and Lim, C. C.: 2006, *Geophys. Astro. Fluid Dyn.* **100**, 1
- Berdichevsky, V.: 1998, *Phys. Rev. E* **57**, 2885
- Berlin, T. H. and Kac, M.: 1952, *Phys. Rev.* **86(6)**, 821
- Brown, L. S.: 1992, *Quantum Field Theory*, Cambridge UP, Cambridge
- Ceperley, D. M.: 1995, *Rev. o. Mod. Phys.* **67**, 279
- DiBattista, M. T. and Majda, A.: 2001, *Th. and Comp. Fluid Dyn.* **14**, 293
- Feynman, R. P. and Wheeler, J. W.: 1948, *Rev. o. Mod. Phys.* **20**, 367
- Flandoli, F. and Gubinelli, M.: 2002, *Prob. Theory & Rel. Fields* **122(2)**, 317
- Hartman, J. W. and Weichman, P. B.: 1995, *Phys. Rev. Lett.* **74(23)**, 4584
- Joyce, G. R. and Montgomery, D.: 1973, *J. Plasma Phys.* **10**, 107
- Kevlahan, N. K.-R.: 2005, *Phys. of Fluids* **17**, 065107
- Klein, R., Majda, A., and Damodaran, K.: 1995, *J. Fluid Mech.* **288**, 201
- Lim, C. and Majda, A.: 2001, *Geophys. Astro. Fluid Dyn.* **94**, 177
- Lim, C. C.: 2006, in *Proc. IUTAM Symp.*, Plenary Talk in Proc. IUTAM Symp., Springer-Verlag, Steklov Inst., Moscow
- Lim, C. C. and Assad, S. M.: 2005, *R & C Dynamics* **10**, 240
- Lim, C. C. and Nebus, J.: 2006, *Vorticity Statistical Mechanics and Monte-Carlo Simulations*, Springer, New York
- Lions, P.-L. and Majda, A. J.: 2000, in *Proc. CPAM*, Vol. LIII, pp 76–142, CPAM
- Majda, A. and Wang, X.: 2006, *Non-linear Dynamics and Statistical Theories for Basic Geophysical Flows*, Cambridge UP, Cambridge
- Maxworthy, T. and Narimousa, S.: 1994, *J. Phys. Oceanography* **24**, 865
- Nordborg, H. and Blatter, G.: 1998, *Phys. Rev. B* **58(21)**, 14556
- Onsager, L.: 1949, *Nuovo Cimento Suppl.* **6**, 279
- Raasch, S. and Etling, D.: 1998, *J. Phys. Oceanography* **28**, 1786
- Schrödinger, E.: 1952, *Statistical Thermodynamics*, Cambridge UP, Cambridge
- Sen, P., Trivedi, N., and Ceperley, D. M.: 2001, *Phys. Rev. Lett.* **86(18)**, 4092
- Tsubota, M., Araki, T., and Barenghi, C. F.: 2003, *Phys. Rev. Lett.* **90**, 205301
- Zee, A.: 2003, *Quantum Field Theory in a Nutshell*, Princeton UP, Princeton